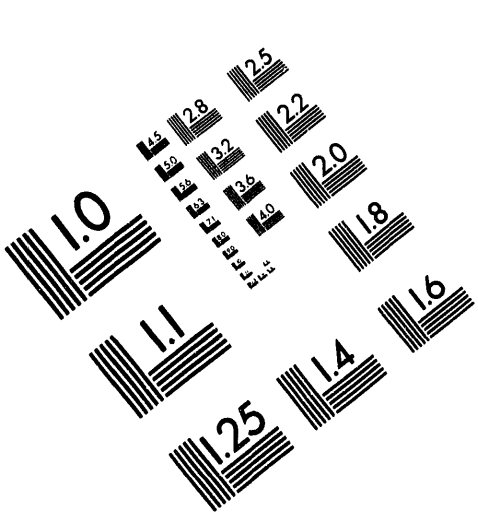

Association for Information and Image Management
1100 Wayne Avenue, Suite 1100
Silver Spring, Maryland 20910
301/587-8202

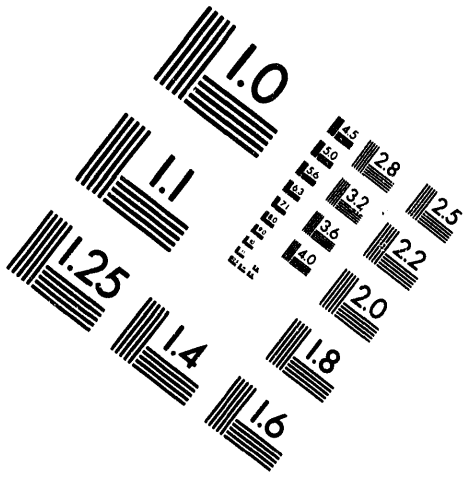

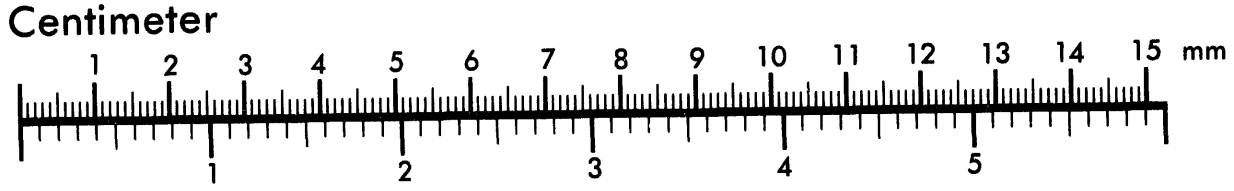

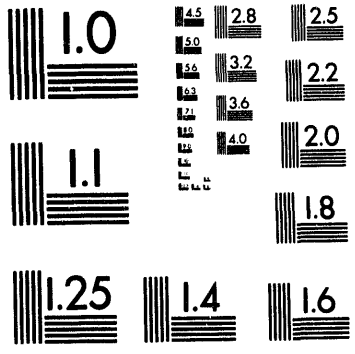

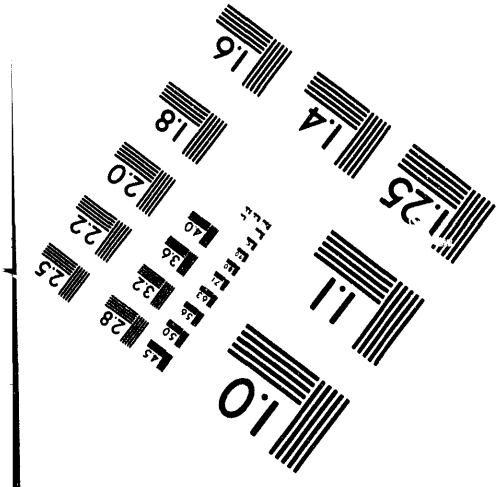

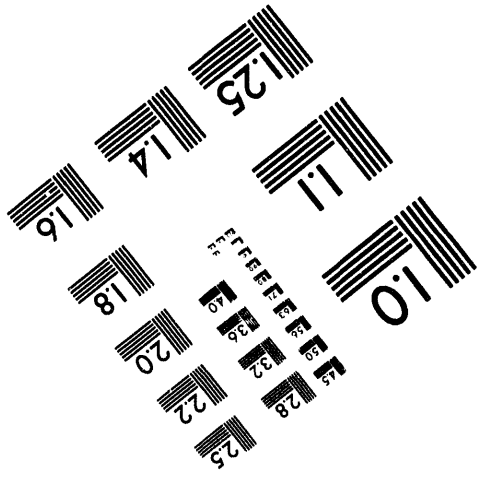

MANUFACTURED TO AIIM STANDARDS
BY APPLIED IMAGE, INC.

1 of 1

CONF-940411--26

Note: This is a preprint of a paper submitted for publication. Contents of this paper should not be quoted or referred to without permission of the author(s).

Submitted for publication in *Epitaxial Oxide Thin Films and Heterostructures*, ed. by D. K. Fork, J. M. Phillips, R. Ramesh, and R. M. Wolf, Materials Research Society, Pittsburgh, Pennsylvania, presented at the Spring Meeting of the Materials Research Society, San Francisco, California, April 4–8, 1994

ATOMIC SCALE STRUCTURE AND CHEMISTRY OF INTERFACES BY Z-CONTRAST IMAGING AND ELECTRON ENERGY LOSS SPECTROSCOPY IN THE STEM

M. M. McGibbon, N. D. Browning, M. F. Chisholm, A. J. McGibbon, S. J. Pennycook, V. Ravikumar,* and V. P. Dravid*

Solid State Division
Oak Ridge National Laboratory
Oak Ridge, Tennessee 37831-6030

*Northwestern University
Department of Materials Science and Engineering
Evanston, Illinois 60208

SOLID STATE DIVISION
OAK RIDGE NATIONAL LABORATORY
Managed by
MARTIN MARIETTA ENERGY SYSTEMS, INC.
under
Contract No. DE-AC05-84OR21400
with the
U.S. DEPARTMENT OF ENERGY
Oak Ridge, Tennessee

May 1994

ATOMIC SCALE STRUCTURE AND CHEMISTRY OF INTERFACES BY Z-CONTRAST IMAGING AND ELECTRON ENERGY LOSS SPECTROSCOPY IN THE STEM

M.M. McGIBBON*, N.D. BROWNING*, M.F. CHISHOLM*, A.J. McGIBBON*, S.J. PENNYCOOK*, V. RAVIKUMAR** AND V.P. DRAVID**
* Solid State Division, Oak Ridge National Laboratory, Oak Ridge, TN 37831-6031, USA
** Northwestern University, Department of Materials Science and Engineering, Evanston, IL 60208, USA

ABSTRACT

The macroscopic properties of many materials are controlled by the structure and chemistry at grain boundaries. A basic understanding of the structure-property relationship requires a technique which probes both composition and chemical bonding on an atomic scale. High-resolution Z-contrast imaging in the scanning transmission electron microscope (STEM) forms an incoherent image in which changes in atomic structure and composition across an interface can be interpreted directly without the need for preconceived atomic structure models (1). Since the Z-contrast image is formed by electrons scattered through high angles, parallel detection electron energy loss spectroscopy (PEELS) can be used simultaneously to provide complementary chemical information on an atomic scale (2). The fine structure in the PEEL spectra can be used to investigate the local electronic structure and the nature of the bonding across the interface (3). In this paper we use the complimentary techniques of high resolution Z-contrast imaging and PEELS to investigate the atomic structure and chemistry of a 25° symmetric tilt boundary in a bicrystal of the electroceramic $SrTiO_3$.

INTRODUCTION

In the VG HB501 UX dedicated STEM, the image is formed by scanning a 2.2Å probe across the specimen. The integrated output from various imaging detectors is displayed on a TV screen scanning at the same rate. The Z-contrast signal is collected from a high angle annular detector where, by collecting the component of the electron signal scattered through large angles (typically 75 to 150 mrad) the resultant image is dominated by thermal diffuse scattering. In this high angle regime lateral coherence between individual columns is destroyed, enabling an incoherent image to be produced with a spatial resolution limited by the size of the scanning probe (4). Provided the incident electron probe is smaller than the lattice spacing (for a sample oriented to a major zone axis) the resultant image will be a map of the columnar scattering power. Furthermore, the relative intensity of scattering from each column reflects the changes in the composition on an atomic scale. For thicker samples, where beam spreading might be expected to degrade the resolution, theoretical calculations (4) have shown that the spatial resolution is preserved by channeling of the electrons down the atomic columns, provided the sample is oriented to a major zone axis. Experiments have confirmed the electron channeling effect in thicker samples (~500Å) where the image merely reduces in contrast as the incident beam becomes depleted by the increasing number of scattering events.

The key aspect of this technique is that intensity distributions in high-resolution Z-contrast images provide a direct image of the atomic column sites which is sensitive to both structure and composition on an atomic scale (5). High resolution CTEM images are more difficult to interpret in such terms since reversals in image contrast as a function of focus and specimen thickness can occur. As the Z-contrast signal is collected from an annular detector, the inelastic signal, which is scattered through significantly lower angles can be collected simultaneously to form an electron energy loss spectrum. Consequently, the high-resolution Z-

contrast image can be used to position the electron probe on specific atomic sites to collect PEELS data.

In order to achieve atomic resolution PEELS microanalysis, the range over which the fast electron can cause a particular excitation or energy loss must be less than the inter-atomic spacing. This interaction can be described classically by an impact parameter (6). Previous work has shown that for energy losses greater than ~300eV and a collection angle of 25 mrad (typical in the work presented here) the impact parameter is sufficiently small that the spatial resolution of the PEELS signal is dominated by the incident probe size of 2.2Å (7). It should be noted that this classical approach is probably an overestimate of the impact parameter since screening of the atomic electrons will further reduce the effective impact parameter (8).

ATOMIC SCALE CHARACTERIZATION OF A $SrTiO_3$ GRAIN BOUNDARY.

$SrTiO_3$ is an important electroceramic material whose electrical properties are controlled by the atomic, chemical and electronic structure at the grain boundary. Figure 1(a) shows a Z-contrast image from a 25° [001] tilt boundary in a $SrTiO_3$ bicrystal. The image was acquired from a cross-sectional specimen oriented in the <100> direction. The brighter spots in the image correspond to the strong scattering power of the heavier Sr columns (Z=38) with the less bright spots corresponding to the lighter Ti columns (Z=22).The Sr atoms have a spacing of 3.9Å in the <100> projection to give an idea of scale on the image in figure 1(a). The lighter O atomic columns are not visible in a Z-contrast image. In figure 1(b) the maximum entropy technique of Gull and Skilling (9) has been applied to enhance the image resolution and to determine the atomic column positions and intensities directly from the image (without the need for preconceived structure models). Figure 2 shows the atomic coordinates of the Sr columns obtained from a central region of the maximum entropy reconstruction, figure 1(b). The average crystal lattice, determined from the coordinates of the Sr columns in a region of the image away from the grain boundary, is shown in figure 2 overlaying the Sr column matrix. This allows us to determine the accuracy of the measured atomic column positions. The statistical error in the maximum entropy calculation of the atomic column positions (~2%) is dominated by a systematic error introduced by a slight tilt in the sample which gives an overall accuracy of ~5% (0.2Å) in the Sr and Ti atomic column positions.

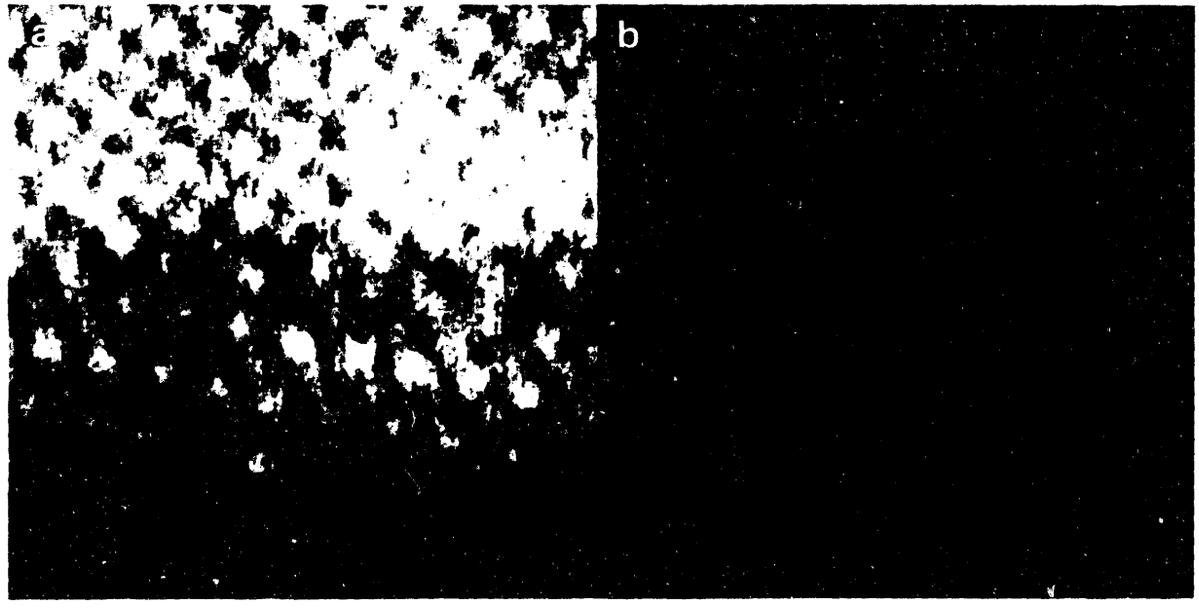

Figure 1 (a) Z-contrast image and (b) maximum entropy processed image of a 25° grain boundary in a $SrTiO_3$ bicrystal.

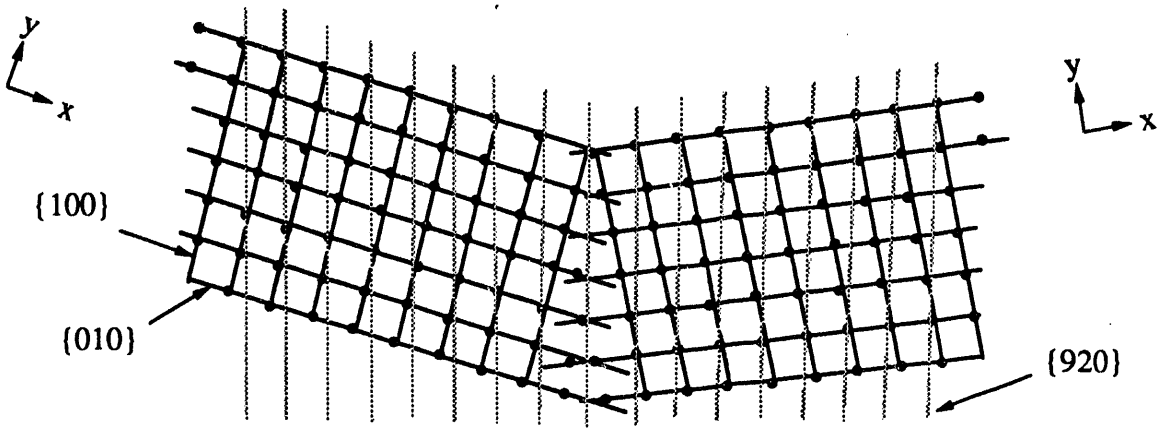

Figure 2. The average crystal lattice, determined from the Sr atomic column coordinates in a region of the image away from the grain boundary, is shown overlaying the Sr column matrix. The corresponding {920} planes in each unit cell, calculated from the average crystal lattice, indicate a grain boundary expansion of ~16%.

The misorientation between the two grains in the bicrystal was measured directly from the maximum entropy reconstruction of figure 1(b) and was found to be $(25\pm1)^{o}$. This corresponds to a $\Sigma=85$ boundary. No rigid body translation is observed along the common (920) boundary plane within the 0.2Å accuracy of the atomic column positions. The corresponding (920) planes for each unit cell were calculated from the average crystal lattice in figure 2 and are shown overlaid. From this sequence of parallel planes a grain boundary expansion of 16.4% was measured. This corresponds to a translation normal to the boundary plane of (0.6±0.2)Å and occurs in a slab of material two unit cells wide and centered on the boundary plane. The systematic error introduced by tilt effects may affect this grain boundary expansion but the extent of expansion observed is still statistically significant.

Although the coordinates of the Sr and Ti columns can be determined directly from the Z-contrast image, there is no information on the position of the O atoms in the grain boundary. However, by using the Z-contrast image to accurately position the probe at the grain boundary for PEELS acquisition, the fine structure within the PEELS edges can be used to investigate the O and Ti bonding at the boundary. Series of Ti and O spectra were acquired at unit cell intervals (~4Å) across a $SrTiO_3$ grain boundary. To reduce the dose on a single atomic column the spectra were acquired while scanning the probe repeatedly along a line parallel to the interface which retains the atomic resolution across the interface. The exposure time for the Ti L_{23} edge was limited to 2s and the O K-edge to 5s to reduce the effects of specimen drift (~2-3Å/min). By collecting 2 spectra at each point it was possible to determine there was no beam damage during these short acquisition times and subsequently it enables the spectra to be added together to improve statistical accuracy.

Figure 3 shows a comparison of the Ti L_{23} edge acquired in the bulk and at the grain boundary. It can be seen that the only significant change between the bulk and boundary spectra is a slight broadening of the peaks in the fine structure of the edge. From molecular orbital calculations the fine structure within the PEELS edges can be assigned as transitions from the core level to the conduction band. The first peak in the Ti L_2 and L_3 edges and the O K edge arises from transitions to a π^* antibonding level and the second peak from transitions to a σ^* antibonding level (10). The higher energy region of the conduction band involves many overlapping transitions and it is not possible to assign a peak in the PEELS edge to an individual transition. Therefore, the broadening of the π^* and the σ^* transitions in the grain boundary spectrum of figure 3 corresponds to a broadening of the energy levels as the Ti-O bonds are distorted across the grain boundary. Previous studies have shown that the fine structure within the Ti L_{23} edge is very sensitive to the coordination of the Ti atoms (11). In particular, a change in coordination of the Ti atoms at the grain boundary would result in an significant change in the fine structure of the Ti edge acquired at the grain boundary in figure 3. Since there is no significant change in the Ti edge at the grain boundary we conclude that the Ti

atoms remain octahedrally coordinated to O across the grain boundary. In addition, previous studies have observed chemical shifts in the PEELS edge energy onset of the order of 1 to 3eV with a change in valency in transition metals (12,13). Since no chemical shift is observed in figure 3, we conclude that the average Ti valency along the grain boundary in $SrTiO_3$ remains 4+ across the grain boundary region. Local probing along the length of the grain boundary shows no significant change in the Ti coordination. Therefore, although the Ti-O bonds themselves may be distorted across the grain boundary the Ti atoms remain octahedrally coordinated to the O atoms in the grain boundary structure.

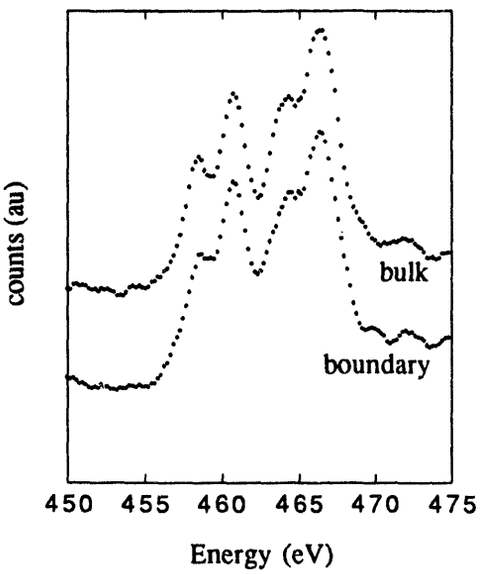

Figure 3. A comparison of Ti L_{23} spectra acquired at the grain boundary and in the bulk of a $SrTiO_3$ bicrystal.

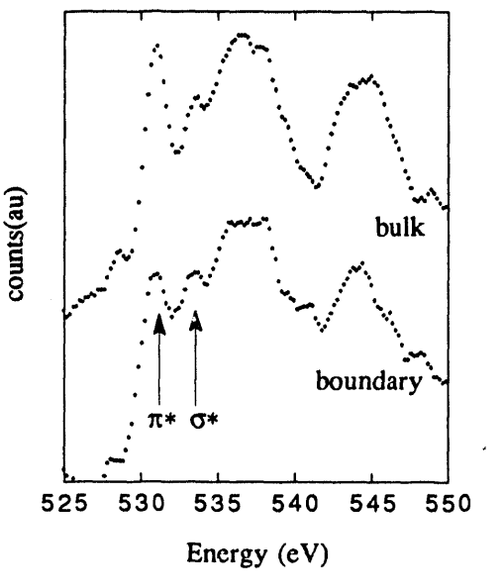

Figure 4. A comparison of O K-edge spectra acquired at the grain boundary and in the bulk of a $SrTiO_3$ bicrystal.

Figure 4 shows a comparison of the O K edge spectra acquired in the bulk and at the grain boundary. From the figure, it is clear that there is an increase in the intensity of the σ^* peak relative to the π^* peak in the grain boundary spectrum. This increase in σ^* transitions may be explained qualitatively by considering the oxygen coordination in $SrTiO_3$ (14). In the linear O-Ti coordination of $SrTiO_3$, shown schematically in figure 5, only the p_x orbitals contribute to the σ bonding. In comparison, in the threefold O-Ti coordination of TiO_2 (rutile), also shown in figure 5, both the p_x and p_z orbitals contribute to the σ bonding thus increasing the σ contribution to the bonding. A corresponding increase in the σ^* peak is observed experimentally in the O edge of TiO_2 compared to the O edge of $SrTiO_3$. In an analogous manner, the increase in the σ^* peak of the grain boundary spectrum in figure 4 suggests that the linear coordination of the O-Ti bonds in $SrTiO_3$ is distorted at the grain boundary producing a larger number of σ^* transitions.

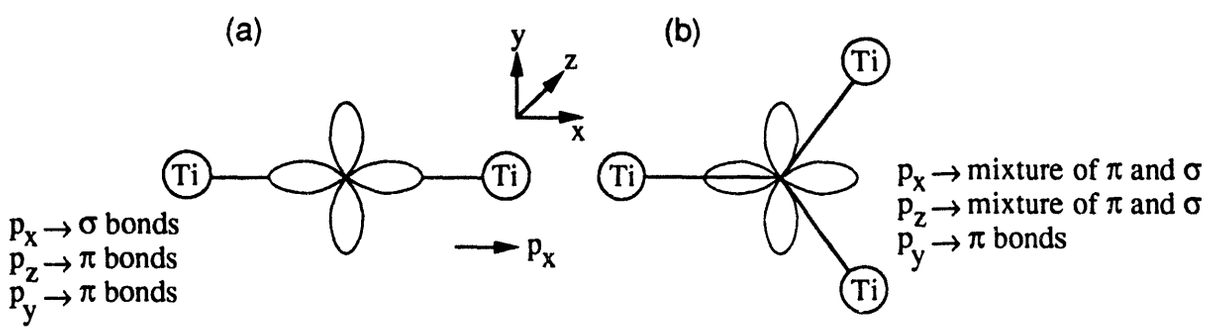

Figure 5. Consideration of molecular orbital contributions to the π and σ bonds in (a) the linear coordination of $SrTiO_3$ and (b) the threefold coordination of TiO_2 (rutile).

We can now combine the information on the Ti-O coordination with the Sr and Ti atomic column positions determined from the Z-contrast image to deduce the boundary structure. The O atoms are added to the grain boundary structure model to maintain the octahedral Ti-O coordination and to preserve charge neutrality in the grain boundary region. Figure 6 shows a single repeat unit of the grain boundary structure calculated by combining the information available from the Z-contrast image and the PEELS.

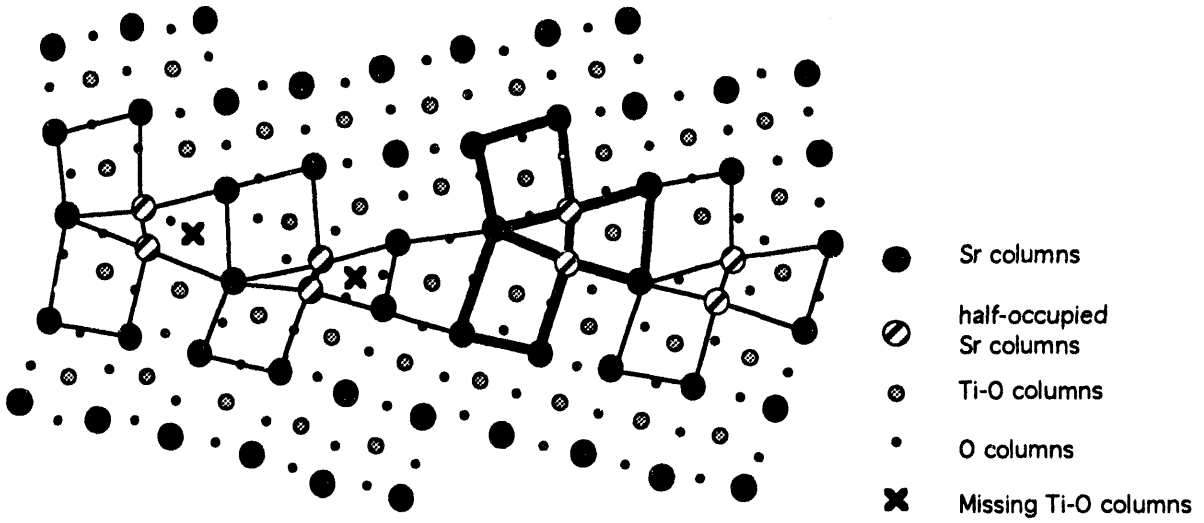

Figure 6. The grain boundary structure model determined by combining the structural information from the Z-contrast image and the Ti-O coordination information from PEELS.

It should be noted however, that the Sr-Sr distance at the base of the Sr triangles in figure 6, which was measured directly from the maximum entropy reconstruction, is significantly below the lowest nearest neighbor distances commonly found for Sr (~3.8Å). One possible explanation for this is that the Sr atoms in these columns lie in alternate planes in the beam direction producing half occupied Sr columns and giving a Sr-Sr spacing of > 4.0Å. Since the Z-contrast image is a planar projection of the 3-dimensional structure it would still image two distinct Sr atomic columns, with reduced intensity as is found experimentally. However, due to the second order effects, such as a possible changes in the atomic vibration amplitude for atoms in the grain boundary and disorder scattering and dechanneling effects due to surface relaxation of strained regions near the boundary, it is not possible to obtain precise atomic column occupancies directly from the Z-contrast image in the grain boundary region.

We tested the validity of this structural model by bond-valence sum calculations (14,15). In these calculations, the contribution that a particular bond makes to the formal valence of each of the atoms involved in the bond can be calculated from the bond length. Using the coordinates of the metal columns determined by the maximum entropy image analysis, the oxygen columns positions were refined so as to maintain charge neutrality with the correct valence on all the atoms. We have assumed the O columns to be straight and the atoms to be confined to their respective planes. It was necessary, in a few isolated cases, to adjust the positions of the metal columns to ensure that the valence on any individual site did not vary by more than 0.5 from the average. However, these movements were less than the 0.2Å positional error in the coordinates. In this manner the average valencies and standard deviations in the structural unit were found to be 2.11±.23 for Sr, 4.08±.24 for Ti and 2.08±.29 for O, which agree well with the values calculated for the bulk material (Sr=2.11, Ti=4.14 and O=2.08). Although bond valence sums cannot determine the reason for the missing Ti-O columns in the structure model of figure 6, it is interesting to note that the Ti-O columns in the adjacent unit cells relax consistent with preserving charge neutrality at the grain boundary.

CONCLUSIONS

By combining the structural information from the Z-contrast image and the bonding information available from the PEELS we have established a grain boundary structure model for a 25° tilt boundary in a $SrTiO_3$ bicrystal directly from the experimental data without the need for preconceived model structures. The half-occupied Sr columns in the grain boundary structure model represent candidate sites for larger dopants (by substitution for Sr), typical of the dopant atoms used in these materials. The Ti and O vacancies in the grain boundary structure may also represent candidate sites for smaller dopant atoms since the surrounding atoms appear able to relax to accommodate the presence or absence of the Ti-O columns. We believe that further structural studies of this type in conjunction with full atomistic calculations could finally reveal how grain boundaries control the macroscopic electrical properties of these materials.

ACKNOWLEDGMENTS

We would like to thank T.C.Estes, J.T.Luck and S.L.Carney for technical assistance. This research was sponsored by the Division of Materials Sciences, US Department of Energy, under contract No. DE-AC05-84OR21400 with Martin Marietta Energy Systems, Inc., and supported in part by an appointment to the Oak Ridge National Laboratory Postdoctoral Research Program administered by the Oak Ridge Institute for Science and Education. VR and VPD are supported by U.S.Department of Energy Grant No. DE-FG02-92ER45475

REFERENCES

(1) S.J. Pennycook and D.E. Jesson, Phys.Rev.Lett, **64**, 938, (1990)
(2) N.D.Browning et al, Nature, **366**, 143 (1993)
(3) P.E.Batson, Nature, **366**,727 (1993)
(4) S.J. Pennycook and D.E. Jesson, Ultramicroscopy, **37**, 14, (1991)
(5) S.J. Pennycook, Annu. Rev. Mater. Sci., **22**, 171, (1992)
(6) S.J.Pennycook, Contemp.Phys, **23**, 371 (1982)
(7) N.D.Browning and S.J.Pennycook, Microbeam Analysis, **2**, 81, (1993)
(8) P.E.Batson, Ultramicroscopy, **47**, 133 (1992)
(9) S.F.Gull and J.Skilling, IEE Proc, **131F**, 646 (1984)
(10) L.A.Grunes et al, Phys.Rev.B, **25**, 7157 (1982)
(11) R.Brydson, H.Sauer and W.Engel, Transmission Electron Energy Loss Spectrometry in Materials Science (The Minerals, Metals and Materials Society) 1992
(12) J.H.Paterson and O.L.Krivanek, Ultramicroscopy, **32**, 319 (1990)
(13) M.T.Otten et al, Ultramicroscopy, **18**, 285, (1985)
(14) R.Brydson et al, J.Phys:Condens.Matter, **4**, 3429 (1992)
(15) D.Altermatt and I.D.Brown, Acta Cryst, **B41**, 240 (1985)
(16) I.D.Brown and D.Altermatt, Acta Cryst, **B41**, 244 (1985)

DATE
FILMED
7/26/94
END